VIP Computational Chemistry

DOI: 10.1002/anie.201205338

The Reaction Coordinate of a Bacterial GH47 α-Mannosidase: A Combined Quantum Mechanical and Structural Approach**

Andrew J. Thompson, Jerome Dabin, Javier Iglesias-Fernández, Albert Ardèvol, Zoran Dinev, Spencer J. Williams, Omprakash Bande, Aloysius Siriwardena, Carl Moreland, Ting-Chou Hu, David K. Smith, Harry J. Gilbert, Carme Rovira, and Gideon J. Davies**

The reaction coordinates of diverse mannosidases are of fundamental mechanistic interest and are increasingly relevant to inform the chemical syntheses of mannosides.[1] Furthermore, the importance of α-mannosidase catalysis in crucial biochemical events, in both the healthy cell and in the context of disease, imparts special relevance to the dissection of enzyme action and the specific inhibition of these enzymes. One particularly important group are the so-called mannosidase I Golgi and endoplasmic reticulum (ER) α-mannosidases, and their homologues, grouped in the sequence-based CAZY[2] family GH47. These enzymes are involved in the biosynthetic "trimming" and/or remodeling of mannose-containing N-glycans, or in their degradation. All characterized GH47 enzymes are inverting α-1,2 mannosidases; the biosynthetic ER enzymes act on $Man_9GlcNAc_2$ glycans (generating $Man_8GlcNAc_2$[3]), while the Golgi enzymes trim the oligosaccharides ultimately into $Man_5GlcNAc_2$;[4] and a third subgroup of ER-located enzymes play roles in the degradation of misfolded proteins as part of the protein folding quality control apparatus.[3a,5]

Insight into the $(\alpha/\alpha)_7$ GH47 fold and the presence of an essential active site Ca^{2+} ion was first provided through the determination of the structure of the yeast *Saccharomyces cerevisiae* class I α-1,2 mannosidase.[6] Subsequently, through studies of the human class I enzyme, a ring-flipped $^1C_4$ conformation was observed for the inhibitor deoxymannojirimycin bound at the active center and mirrored in the conformation of the bound bicyclic inhibitor, kifunensine.[7] The Michaelis complex of the human enzyme, formed with an S-linked disaccharide substrate mimic (**1**), was observed in a $^3S_1$ conformation,[3b] an observation later corroborated by docking calculations.[8] Together these data supported a conformational coordinate for GH47 enzymes, potentially through a $^3H_4$ conformation at, or close to, the transition state. An understanding of the conformation of the transition state is important in efforts to develop inhibitors based on the concept of transition state mimicry; this is of great interest in developing reagents to study the intersection of pathways involving N-glycan maturation and remodeling as well as degradation and disposal.

Herein, we present the structural analysis of Michaelis, transition state, and product mimicking complexes with a bacterial GH47 α-mannosidase, from *Caulobacter* strain K31, which we show shares the specificity of the human GH47 enzymes for α-1,2 glycans. *Caulobacter* GH47 crystals diffract to sub-Ångström resolution (Table 1), thus allowing exquisite atomic resolution analysis of ligand distortion: the Michaelis complex of the S-linked substrate mimic **1** reveals the equivalent distortion seen previously for the human orthologue,[3b] whereas novel complexes with the inhibitors manno-

[*] A. J. Thompson, Dr. J. Dabin, Dr. T.-C. Hu, D. K. Smith, Prof. G. J. Davies
Department of Chemistry, University of York
Heslington, York, YO10 5DD (UK)
E-mail: gideon.davies@york.ac.uk

J. Iglesias-Fernández, Dr. A. Ardèvol, Prof. C. Rovira
Computer Simulation & Modeling Laboratory
Parc Científic de Barcelona
Baldiri Reixac 4, 08028 Barcelona (Spain)
and
Institut de Química Teòrica i Computacional (IQTCUB) (Spain)
E-mail: crovira@pcb.ub.es

J. Iglesias-Fernández, Prof. C. Rovira
Present address: Departament de Química Orgànica
Universitat de Barcelona
Martí i Franquès 1, 08028 Barcelona (Spain)

Dr. A. Ardèvol
Present address: Department of Chemistry and Applied Biosciences, ETH Zurich, USI Campus
Via Giuseppe Buffi 13, CH-6900 Lugano (Switzerland)

Prof. C. Rovira
Institució Catalana de Recerca i Estudis Avançats (ICREA)
Passeig Lluís Companys 23, 08020 Barcelona (Spain)

Dr. Z. Dinev, Assoc. Prof. S. J. Williams
School of Chemistry and Bio21 Molecular Science and Biotechnology Institute, University of Melbourne
Parkville (Australia)

Dr. O. Bande, Dr. A. Siriwardena
Université de Picardie Jules Vernes, Laboratoire des Glucides (CNRS-FRE 3617), 33, Rue Saint Leu, 80039 Amiens (France)

C. Moreland, Prof. H. J. Gilbert
Institute for Cell and Molecular Biosciences
The Medical School, Newcastle University
Framlington Place, Newcastle upon Tyne, NE2 4HH (UK)

[**] We thank the UK Biotechnology and Biological Sciences Research Council (BBSRC), the Spanish Ministry of Economy and Competitiveness (MINECO, CTQ2011-25871), and the Generalitat de Catalunya (2009SGR-1309). A.S. thanks the Indo-French Centre for the Promotion of Advance Research (IFCPAR/CEFIPRA) for funding and for a postdoctoral fellowship (to O.B.). A.A. acknowledges a long-term fellowship from the European Molecular Biology Organization (EMBO). We acknowledge the computer support, technical expertise, and assistance provided by the Barcelona Supercomputing Center: Centro Nacional de Supercomputación (BSC-CNS).

Supporting information for this article is available on the WWW under http://dx.doi.org/10.1002/anie.201205338.

Table 1: 3D structure data for *Ck*GH47.[a]

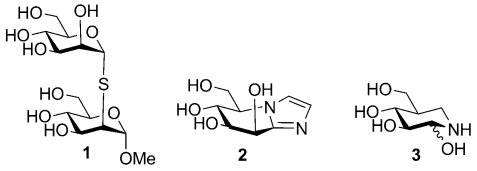

	Native	1	2	3
resolution [Å]	50–0.85	50–0.85	50–1.10	50–1.10
R_{merge}	0.04 (0.39)	0.04 (0.57)	0.07 (0.28)	0.04 (0.21)
I/sigma	17.9 (2.6)	16.9 (1.7)	18.7 (5.4)	32.2 (6.7)
comp. [%]	91.9 (63.4)	97.2 (80.8)	99.2 (94.2)	89.6 (49.5)
R_{cryst}/R_{free}	0.097/0.11	0.097/0.11	0.089/0.11	0.083/0.10
$rmsd_{bonds}$	0.009	0.010	0.010	0.010
$rmsd_{angles}$	1.39	1.43	1.39	1.39
PDB Code	4AYO	4AYP	4AYQ	4AYR

[a] Values in parentheses denote highest resolution shell.

imidazole **2** and noeuromycin **3** allow the definition of a complete conformational coordinate in which the mannoside passes from a Michaelis complex in the $^3S_1$ conformation via a $^3H_4$ transition state to product bound in a $^1C_4$ conformation. Crucially, these atomic resolution analyses inform a quantum mechanical description of the conformational sphere of α-D-mannopyranose, presenting for the first time the southern hemisphere, which is of direct relevance to GH47 α-mannosidase catalysis. Quantum mechanical calculations show that the free energy landscape (FEL) of the isolated α-D-mannopyranose molecule is strongly perturbed on-enzyme and is restricted to a single conformational pathway for the enzyme-bound ligand that is entirely consistent with the experimentally supported $^3S_1 \rightarrow {}^3H_4 \rightarrow {}^1C_4$ catalytic conformational progression.

To obtain a GH47 model that is easily produced and diffracts to near atomic resolution a variety of enzymes were studied. The gene encoding the bacterial GH47 from *Caulobacter* strain K31 (*Ck*GH47) was synthesized in a codon-optimized form for expression in *Escherichia coli* (see the Supporting Information). The enzyme was inactive on a range of aryl α-D-mannosides, but kinetics could be determined through fluoride-release using α-D-mannosyl fluoride (Supporting Information, Figure S2). This substrate yielded $k_{cat} = 1.9\ s^{-1}$ and $K_M = 5.0$ mM with $k_{cat}/K_M = 0.38\ s^{-1}\,mM^{-1}$, thus allowing determination of a pH optimum of approximately 7.0. Screening of a range of mannose-disaccharides at the pH optimum showed *Ck*GH47 to be an α-1,2-mannosidase with $k_{cat} = 111 \pm 3\ min^{-1}$ and $K_M = 120 \pm 7$ μM [$k_{cat}/K_M = 0.93\ min^{-1}\,\mu M^{-1}$ ($15.4\ s^{-1}\,mM^{-1}$)] against α-1,2-mannobiose, with no observable activity against all other linkages, which is consistent both with the activity of the eukaryotic enzymes and also with a complex subsequently obtained with **1**, as discussed below. Working at the pH optimum, *Ck*GH47 α-mannosidase was inhibited by **1, 2**, and **3** with K_D values of 755 nM, 47 nM, and 99 nM respectively, as determined by isothermal titration calorimetry (Figure S3).

Crystals of the *Caulobacter* GH47 enzyme diffract to atomic (≤1 Å) resolution. Apo-enzyme structures, as well as those with **1**–**3** defining the reaction coordinate, were solved to resolutions of 0.85, 0.85, 1.10, and 1.10 Å, respectively (Figure 1). As for previously solved mammalian orthologues, the native structure of *Ck*GH47 is an $(\alpha/\alpha)_7$ helical barrel with the catalytic center featuring the essential Ca^{2+} ion in a closed cavity. Uniquely however, this bacterial orthologue also coordinates a second Ca^{2+} located approximately 6.5 Å from the first at the base of the active site pocket, the relevance of which, if any, is unclear. The reaction coordinate was studied through complexes of **1**–**3**. The non-hydrolyzable disaccharide **1**, binds in the −1 and +1 subsites with the −1 subsite mannoside distorted to an $^{3,O}B$ / $^3S_1$ conformation (**1**; Figure 1). The active center Ca^{2+} ion bridges O2 and O3 of the mannoside, thus facilitating ring distortion (to yield an O2-C2-C3-O3 torsion angle of 47°) with the putative nucleophilic water aligned for in-line attack (water-C1-S1 angle of 155°). This water interacts both with the active center Ca^{2+} and the putative catalytic base, Glu365 (distances 2.4 and 2.7 Å, respectively). As with the human enzyme complex formed with **1**, the putative catalytic acid does not interact directly with the interglycosidic atom with a Glu121 OE2–S1 distance

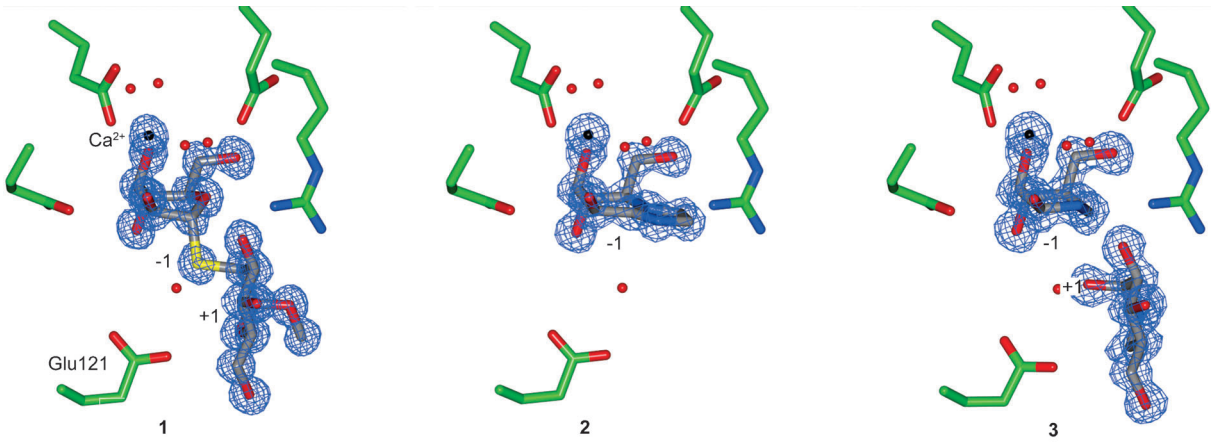

Figure 1. Observed electron density for **1**–**3** bound to Caulobacter Strain K31 α-1,2-mannosidase at 0.85–1.1 Å resolution. The conformations observed are the $^{3,O}B/^3S_1$ conformation for substrate mimic **1**, the $^3H_4$ conformation for the putative transition state, mannoimidazole **2**, and $^1C_4$ for noeuromycin **3**, the observed conformation of which mimics that seen in the product.

of 4.5 Å, which suggests an indirect protonation event, perhaps through a water molecule. Given the atomic resolution of the diffraction data, not only are many of the "riding" hydrogen atoms observable but also the hydrogen atoms of the O4 and O6 hydroxy groups of the −1 subsite sugar, allowing an unprecedented level of detail of the substrate interactions of this class of enzyme.

Complexes were also obtained with mannoimidazole **2** and noeuromycin **3**. Mannoimidazole **2** is a putative transition state mimic and binds in a $^{3}H_{4}$ conformation, which provides evidence for the transition state conformation. In solution, noeuromycin **3** exists in α- and β-configured hemiaminal forms (1:2 D-*manno*/D-*gluco* configurations),[9] **3** binds to *Ck*GH47 as the less favored D-*manno*-configured hemiaminal in a ring-flipped $^{1}C_{4}$ conformation, which mimics the product. The major difference between the $^{3,O}B/^{3}S_{1}$ conformation of the substrate mimic **1**, the $^{3}H_{4}$ conformation of the putative transition state mimic **2**, and the $^{1}C_{4}$ conformation of the product mimic **3** is the position of the (pseudo)anomeric carbon. The change in the position of this atom is consistent with the electrophilic migration of C1 from the glycosidic oxygen to the nucleophilic water along the substitution reaction coordinate.

Previous computational studies on β-D-glucopyranose, β-D-mannopyranose, and α-L-fucopyranose have revealed that the isolated sugar can access only a small number of possible conformational coordinates, as reflected in lower free energy states. However, individual enzyme families select only one of these possible routes.[10] For α-D-mannopyranose (Figure 2a) conformations $B_{2,5}$, $^{O}S_{2}$, $^{3,O}B$, $^{3}S_{1}$, $B_{1,4}$, $^{5}S_{1}$, and $^{2,5}B$ (center of the diagram), as well as $^{4}C_{1}$, are among the most stable. Moreover, these conformations were found to be preactivated for catalysis in terms of energy, anomeric charge, and structural parameters (see Figure S8 for the preactivation index). The observed conformations for pseudo-Michaelis complexes in α-mannosidases ($^{O}S_{2}$ and $^{3}S_{1}$ in retaining and inverting enzymes, respectively) are among the most stable and thus represent preactivated conformations. GH125 inverting α-mannosidases show no substrate distortion in their pseudo-Michaelis complex and whereas the conformational pathway for GH125 is unclear, it is certainly consistent with an initial $^{4}C_{1}$ conformation as this is one of the most preactivated conformations identified here (see the Supporting Information).[11]

To quantify how GH47 α-1,2-mannosidases restrict the substrate conformational landscape, metadynamic calculations were repeated using the substrate α-1,2-mannobiose, starting from the crystallographically-determined Michaelis complex (the sulfur atom of the S-linked disaccharide **1** was computationally replaced by oxygen). As shown in Figure 2b, the enzyme acts to fundamentally restrict the energetically accessible conformational landscape of the −1 α-mannosyl residue. Of particular note, the undistorted $^{4}C_{1}$ conformer is no longer an energy minimum. On enzyme, the $^{3,O}B/^{3}S_{1}$ conformations are the only stable distorted conformations, defining a clear $^{3,O}B/^{3}S_{1}\rightarrow{}^{3}H_{4}\rightarrow{}^{1}C_{4}$ conformational pathway for the reaction coordinate, Scheme 1. Both energy minima (corresponding to $^{3,O}B/^{3}S_{1}$ and $^{1}C_{4}$ conformations) are almost of the same stability, although the former is approximately

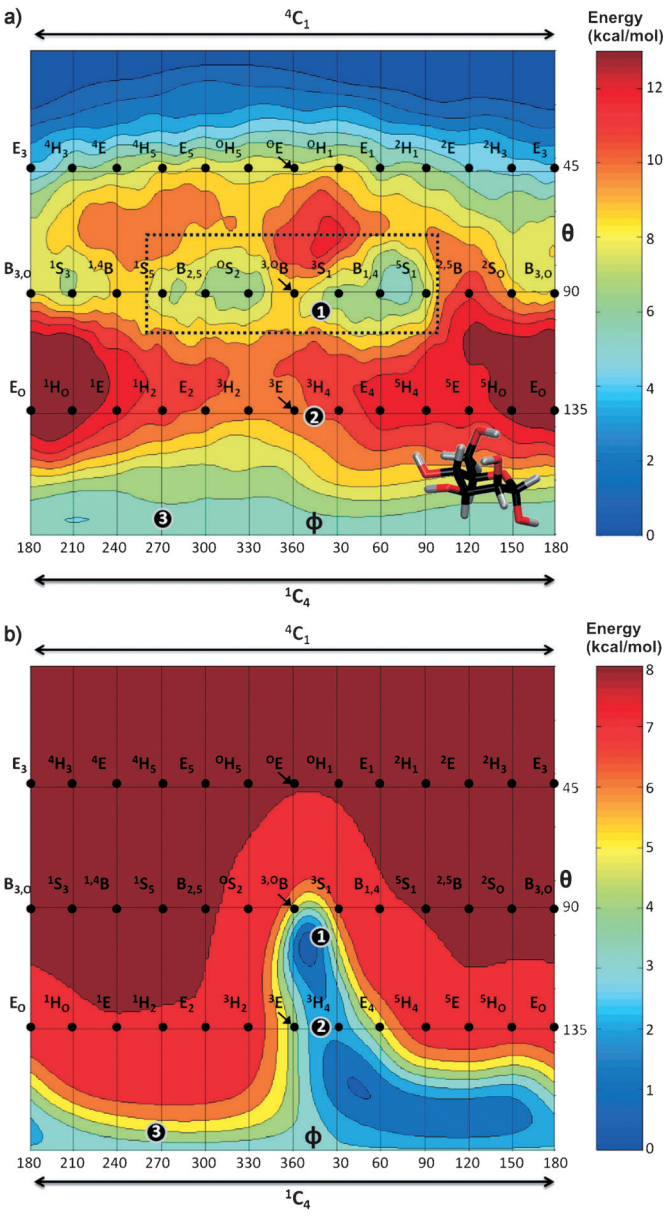

Figure 2. a) Conformational free energy landscape (FEL) of isolated α-D-mannopyranose (Mercator projection including both northern and southern hemispheres); contoured at 1 kcal mol^{-1}. b) Conformational FEL of the α-mannosyl residue at the −1 enzyme subsite of *Caulobacter* α-1,2-mannosidase, contoured at 1 kcal mol^{-1}. Symbols plot the observed conformations of **1**, **2**, and **3**.

0.5 kcal mol^{-1} more stable and wider. This indicates a conformational equilibrium between these two structures in the Michaelis complex; however, nucleophilic substitution can only occur through $^{3,O}B/^{3}S_{1}$ conformations, as only in these conformations is the C1–H bond in a pseudo-equatorial orientation. Bonding differences associated with the sulfur/oxygen linkage and aglycon interactions with the +1 subsite likely favor the $^{3,O}B/^{3}S_{1}$ distorted conformation observed for **1**.

The strategy of using an S-linked substrate mimic with wild-type enzyme has been widely used in the conformational study of the Michaelis complexes of glycoside hydrolases

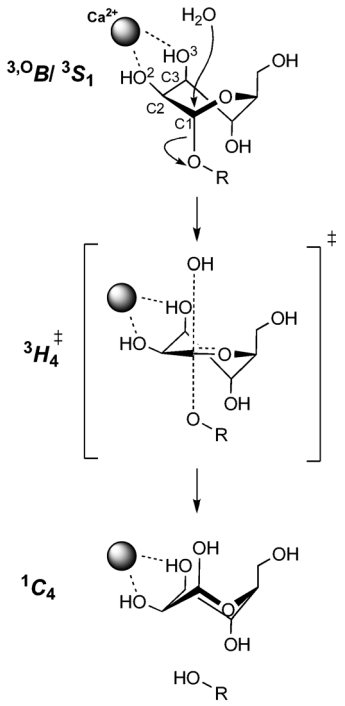

Scheme 1. Reaction coordinate for inverting GH47 α-mannosidases[3b] via a $^3H_4$ transition state. Partial atom numbering is shown for reference and Ca^{2+} is shown as a sphere.

(GHs). The QM/MM optimized structure of the Michaelis complex with the natural substrate is in excellent agreement with the experimental X-ray structure of the Michaelis complex with the S-linked disaccharide substrate mimic **1** (see the Supporting Information), and displays the reactive conformation expected for an inverting GH, as well as a water molecule ideally oriented for in-line nucleophilic attack on the anomeric carbon.

Mannoimidazole **2** has special features that make it an illuminating probe of mannosidase reaction coordinates, including the presence of an sp^2-hybridized (pseudo)anomeric carbon, and the ability to easily adopt the flattened boat and half-chair conformations expected for oxocarbenium-ion-like transition states. For GH2 retaining β-mannosidases, **2** and its derivatives have been observed in a $B_{2,5}$ conformation, with linear free energy relationships showing an almost perfect correlation between the free energy of the binding of the inhibitor ($\log K_I$) and the free energy of the binding of the transition state ($\log K_M/k_{cat}$).[12] This suggests that this conformation mimics that of the transition state, and supports a $^1S_5$ to $B_{2,5}$ to $^OS_2$ progression for the first half of the reaction coordinate. Similarly, **2** was bound in a $B_{2,5}$ conformation to a GH92 inverting α-mannosidase, which is indicative of a $^OS_2 \rightarrow B_{2,5} \rightarrow {}^1S_5$ conformational progression; this observation is consistent with the reverse of that seen for the glycosylation half-reaction of GH2.

In summary, species **2** was found to bind in a $^3H_4$ conformation on GH47, exactly as previously proposed for the GH47 transition state. This is supported by both computational and structural approaches. The bound conformation determined for this one compound alone is diagnostic not only for the transition state conformation, but also for the conformational coordinate of catalysis. This may offer a direct signature allowing assignment of the conformational itinerary of D-*manno*-active enzymes in future structural analyzes. The combination of atomic resolution structural analysis with QM/MM methods allows unparalleled insight into the conformational pathway of a southern hemisphere α-mannosidase. The narrowing (indeed, funneling) of the accessible conformational free energy surface when the enzyme structure is imposed on the surface for free α-D-mannose indicates a single reaction coordinate conformational progression for the GH47 family; one consistent with known 3D structures of this class of enzyme.

Experimental Section

Crystals of *Ck*GH47 were grown as described in the Supporting Information with 3D structures determined by molecular replacement using data collected at beamlines I03, I04, and I041 of the Diamond Light Source (UK). Further details on structure solution and refinement are included in the PDB headers and the Supporting Information. Mannosidase activity was determined both using disaccharide substrates and α-mannosyl fluoride, as described in the Supporting Information. α-mannosyl fluoride (ManF) was synthesized by fluorination of per-*O*-acetylated mannose with HF/pyridine followed by deprotection with catalytic sodium methoxide in methanol, as described previously.[13]

Thermodynamic studies of inhibitor binding, which were determined at the optimal pH for catalysis (pH 7.0), were performed using a MicroCal iTC_{200} calorimeter. Assays were carried out at 25 °C with compounds **1**, **2**, and **3** (all at 500 μM) titrated into the ITC cell containing 50 μM *Ck*GH47. Dissociation constants (K_D) were calculated for each assay using the Origin 7 software package (MicroCal).

Quantum mechanical calculations were performed using Density Functional Theory-based molecular dynamics (MD), according to the Car-Parrinello method.[14] The Kohn–Sham orbitals were expanded in a plane wave (PW) basis set with a kinetic energy cutoff of 80 Ry. The Perdew, Burke, and Ernzerhoff generalized gradient-corrected approximation (PBE)[15] was selected in view of its good performance in previous work on isolated sugars,[16] glycosidases,[17] and glycosyltransferases.[18] The metadynamics algorithm[19] was used to explore the conformational free energy landscape of α-D-mannopyranose, taking as collective variables two of the puckering coordinates of Cremer and Pople[20] (θ,ϕ), in the spirit of the pioneering work by Dowd, French, and Reilly.[21] QM/MM calculations of α-1,2-mannosidase in complex with α-1,2-D-mannobiose were performed using the method developed by Laio et al.,[22] which combines Car-Parrinello MD, with force-field MD. The α-1,2-D-mannobiose and the calcium cation were treated quantum-mechanically, whereas the AMBER force field[23] was used for the rest of the protein and the solvent. The electrostatic interactions between the QM and MM regions were handled by a fully Hamiltonian coupling scheme, wherein the short-range electrostatic interactions between the QM and the MM regions are explicitly taken into account for all atoms[22] (see the Supporting Information for further details).

Received: July 6, 2012
Published online: September 26, 2012

Keywords: computational chemistry · conformation analysis · enzyme mechanisms · glycosidase inhibitor · mannose

[1] D. Crich, *Acc. Chem. Res.* **2010**, *43*, 1144 – 1153.

[2] B. L. Cantarel, P. M. Coutinho, C. Rancurel, T. Bernard, V. Lombard, B. Henrissat, *Nucleic Acids Res.* **2009**, *37*, D233 – 238.
[3] a) Y. Wu, M. T. Swulius, K. W. Moremen, R. N. Sifers, *Proc. Natl. Acad. Sci. USA* **2003**, *100*, 8229 – 8234; b) K. Karaveg, A. Siriwardena, W. Tempel, Z. J. Liu, J. Glushka, B. C. Wang, K. W. Moremen, *J. Biol. Chem.* **2005**, *280*, 16197 – 16207.
[4] a) Y. D. Lobsanov, F. Vallee, A. Imberty, T. Yoshida, P. Yip, A. Herscovics, P. L. Howell, *J. Biol. Chem.* **2002**, *277*, 5620 – 5630; b) W. Tempel, K. Karaveg, Z.-J. Liu, J. Rose, B.-C. Wang, K. W. Moremen, *J. Biol. Chem.* **2004**, *279*, 29774 – 29786.
[5] a) S. W. Mast, K. W. Moremen in *Glycobiology*, *Vol. 415* (Ed.: M. Fukuda), Elsevier, London, **2006**, pp. 31 – 46; b) K. W. Moremen, M. Molinari, *Curr. Opin. Struct. Biol.* **2006**, *16*, 592 – 599.
[6] F. Vallée, F. Lipari, P. Yip, B. Sleno, A. Herscovics, P. L. Howell, *EMBO J.* **2000**, *19*, 581 – 588.
[7] F. Vallee, K. Karaveg, A. Herscovics, K. W. Moremen, P. L. Howell, *J. Biol. Chem.* **2000**, *275*, 41287 – 41298.
[8] a) C. Mulakala, W. Nerinckx, P. J. Reilly, *Carbohydr. Res.* **2006**, *341*, 2233 – 2245; b) C. Mulakala, W. Nerinckx, P. J. Reilly, *Carbohydr. Res.* **2007**, *342*, 163 – 169; c) D. Cantú, W. Nerinckx, P. J. Reilly, *Carbohydr. Res.* **2008**, *343*, 2235 – 2242.
[9] H. Liu, X. Liang, H. Sohoel, A. Bulow, M. Bols, *J. Am. Chem. Soc.* **2001**, *123*, 5116 – 5117.
[10] For a review, see: G. J. Davies, A. Planas, C. Rovira, *Acc. Chem. Res.* **2012**, *45*, 308 – 316.
[11] K. J. Gregg, W. F. Zandberg, J. H. Hehemann, G. E. Whitworth, L. H. Deng, D. J. Vocadlo, A. B. Boraston, *J. Biol. Chem.* **2011**, *286*, 15586 – 15596.
[12] L. N. Tailford, W. A. Offen, N. L. Smith, C. Dumon, C. Morland, J. Gratien, M.-P. Heck, R. V. Stick, Y. Blériot, A. Vasella, H. J. Gilbert, G. J. Davies, *Nat. Chem. Biol.* **2008**, *4*, 306 – 312.
[13] M. Hayashi, S.-I. Hashimoto, R. Noyori, *Chem. Lett.* **1984**, 1747 – 1750.
[14] R. Car, M. Parrinello, *Phys. Rev. Lett.* **1985**, *55*, 2471 – 2474.
[15] J. P. Perdew, K. Burke, M. Ernzerhof, *Phys. Rev. Lett.* **1996**, *77*, 3865 – 3868.
[16] a) X. Biarnés, A. Ardèvol, A. Planas, C. Rovira, A. Laio, M. Parrinello, *J. Am. Chem. Soc.* **2007**, *129*, 10686 – 10693; b) A. Ardèvol, X. Biarnés, A. Planas, C. Rovira, *J. Am. Chem. Soc.* **2010**, *132*, 16058 – 16065.
[17] a) X. Biarnés, J. Nieto, A. Planas, C. Rovira, *J. Biol. Chem.* **2006**, *281*, 1432 – 1441; b) X. Biarnés, A. Ardèvol, J. Iglesias-Fernandez, A. Planas, C. Rovira, *J. Am. Chem. Soc.* **2011**, *133*, 20301 – 20309; c) L. Petersen, A. Ardèvol, C. Rovira, P. J. Reilly, *J. Am. Chem. Soc.* **2010**, *132*, 8291 – 8300; d) I. J. Barker, L. Petersen, P. J. Reilly, *J. Phys. Chem. B* **2010**, *114*, 15389 – 15393.
[18] A. Ardèvol, C. Rovira, *Angew. Chem.* **2011**, *123*, 11089 – 11093; *Angew. Chem. Int. Ed.* **2011**, *50*, 10897 – 10901.
[19] A. Laio, M. Parrinello, *Proc. Natl. Acad. Sci. USA* **2002**, *99*, 12562 – 12566.
[20] D. Cremer, J. A. Pople, *J. Am. Chem. Soc.* **1975**, *97*, 1354 – 1358.
[21] M. K. Dowd, A. D. French, P. J. Reilly, *Carbohydr. Res.* **1994**, *264*, 1 – 19.
[22] A. Laio, J. VandeVondele, U. Rothlisberger, *J. Chem. Phys.* **2002**, *116*, 6941 – 6947.
[23] D. A. Pearlman, D. A. Case, J. W. Caldwell, W. S. Ross, T. E. Cheatham, S. Debolt, D. Ferguson, G. Seibel, P. Kollman, *Comput. Phys. Commun.* **1995**, *91*, 1 – 41.

